

The three-boson system at next-to-leading order in an effective field theory for systems with a large scattering length

Chen Ji,^{1,*} Daniel R. Phillips,^{1,†} and Lucas Platter^{2,3,‡}

¹*Department of Physics and Astronomy,
Ohio University, Athens, OH 45701, USA*

²*Institute for Nuclear Theory, University of Washington, Seattle, WA 98195, USA*

³*Fundamental Physics, Chalmers University of Technology, 412 96 Göteborg, Sweden*

(Dated: March 22, 2012)

Abstract

We analyze how corrections linear in the effective range, r_0 , affect quantities in the three-body sector within an effective field theory for short-range interactions. We demonstrate that observables can be obtained straightforwardly using a perturbative expansion in powers of r_0 . In particular, we show that two linear-in- r_0 counterterms are needed for renormalization at this order if scattering-length-dependent observables are considered. We exemplify the implications of this result using various three-body observables. Analytic results for the running of the next-to-leading-order portion of the three-body force in this effective field theory are provided. Expressions which incorporate $O(r_0)$ corrections and relate the positions of features observed in three-atom recombination near a Feshbach resonance are presented.

*Electronic address: jichen@phy.ohiou.edu

†Electronic address: phillips@phy.ohiou.edu

‡Electronic address: platter@chalmers.se

I. INTRODUCTION

Symmetries are one of the most important concepts in modern-day physics. They are the foundation of the standard model and are also frequently used as a basis for building new physical theories. Even if a symmetry is only approximately fulfilled it can, nonetheless, serve as a starting point for a systematic description of physical observables, since the symmetry breaking effects may be accounted for perturbatively. This approach has been successfully employed in various effective field theories (EFTs) which are low-energy expansions in the ratio of a small parameter over a large parameter. The small parameter is frequently a small momentum and/or energy associated with explicit symmetry breaking. A prominent example of such an EFT is the chiral EFT, whose starting point is the chiral limit of QCD. In this limit, pions are the Nambu-Goldstone bosons associated with the spontaneously broken chiral symmetry of QCD. In the chiral EFT the effect of the nonzero (up, down, and strange) quark masses is then systematically included order-by-order in the low-energy expansion.

While the use of symmetries to constrain theories is usually associated with particle physics, or possibly many-body physics, it has also become important in other fields, such as non-relativistic few-body physics. One example of an important symmetry in this area is discrete scale invariance. Vitaly Efimov showed in 1970 that the non-relativistic three-body system displays discrete scale invariance if the two-body scattering length is large and the range of the interaction is zero [1]. One well-known consequence is that in the limit of infinite scattering length the ratio of the binding energies of two successive three-body bound states is approximately 515.

Efimov also pointed out that his results apply to systems where the two-body scattering length, a , obeys $|a| \gg \ell$, with ℓ the natural length-scale of the two-body potential [1]. They are therefore relevant for a number of systems. One example is nucleon-nucleon scattering, where the scattering length is large compared to the range of the internucleon interaction. A second is provided by manipulation of the atom-atom scattering length of trapped atoms by an external magnetic field such that the atomic scattering displays a Feshbach resonance. Few-body systems of nucleons and atoms, all with interactions tuned such that a shallow two-body bound state is present, will therefore display discrete scale invariance or the remainders of this symmetry. For a recent review of this topic see, e.g., Ref. [2].

Efimov's results have now been rederived as the leading-order (LO) prediction of an

EFT containing only short-range interactions [3, 4]. At LO this EFT corresponds to the Efimovian, large- a , $\ell = 0$ limit. We therefore refer to it hereafter as short-range EFT (SREFT). The contribution of each subsequent order in the SREFT expansion is suppressed by an additional power of ℓ/a , with the first corrections that have to be included in this EFT being those resulting from a finite two-body effective range, r_0 . The effects of these corrections have been analyzed over the last years in a number of works [5–7]. In these studies effective-range corrections were considered for systems in which the scattering length remains fixed. A full analysis requires, however, that we allow for a variable scattering length. Such an analysis was reported in [8, 9]. In this paper we lay out the derivation of the results reported in [9]. We discuss the renormalization of the SREFT in the three-body sector at next-to-leading order (NLO) in the ℓ/a expansion. We show that if, and only if, scattering-length-dependent observables are considered, an additional three-body counterterm is required for renormalization at next-to-leading order. The analysis of Ref. [8] overlooked this result since the combination of the non-perturbative treatment of effective-range corrections and the cutoffs $\Lambda \gg 1/r_0$ employed there modifies the ultraviolet properties of the theory. The results of Ref. [8] therefore are strict EFT predictions only in the limit $|r_0| \gg \ell$.

In Sec. II we will introduce SREFT and briefly review what is known about the two-body sector up to next-to-leading order. We then discuss, in Sec. III, the so-called modified Skorniakov-Ter-Martirosian integral equation which constitutes the application of the SREFT to the three-body sector at leading order. Section IV describes how NLO corrections affect a variety of three-body observables. Section V discusses the running of the NLO parts of the three-body force, and presents analytic results for these counterterms’ renormalization-group evolution. Finally, Sec. VI presents relations between observables measured in three-atom recombination which incorporate effects that are NLO in SREFT. We end with a summary and outlook.

II. THE EFT FOR SHORT-RANGE INTERACTIONS

We employ the SREFT that describes non-relativistic particles interacting through a finite-range interaction with a large scattering length. The inverse of the range of the interaction sets the breakdown scale for this EFT, which is constructed from contact interactions

alone. In nuclear physics this EFT is also known as the pionless EFT (see Refs. [10, 11] for reviews). However, the SREFT can also describe other systems such as atoms close to a Feshbach resonance. Since we perform our analysis for identical bosons we will refer to the interacting particles as atoms.

At the heart of any EFT lies the Lagrangian. It includes all possible interaction terms that are allowed by the symmetries of the underlying interaction and is built from fields that correspond to the degrees of freedom included in the EFT. The SREFT in its original form is therefore built from atom fields alone, however, it has proven useful to employ a Lagrangian that contains a dimer field. The relation between these forms of the Lagrangian is elucidated in Refs. [4, 12–14]. In these works the dimer field is sometimes chosen to be static, sometimes dynamic. The latter version is particularly convenient for the inclusion of effective range corrections, and so we will work with this form of the SREFT Lagrangian, written as:

$$\mathcal{L} = \psi^\dagger \left(i\partial_0 + \frac{\nabla^2}{2m} \right) \psi + \sigma T^\dagger \left(i\partial_0 + \frac{\nabla^2}{4m} - \Delta \right) T - \frac{g}{\sqrt{2}} (T^\dagger \psi \psi + \text{h.c.}) + h T^\dagger T \psi^\dagger \psi + \dots, \quad (1)$$

where the ellipses represent additional higher-order interactions which are suppressed at low momenta. As pointed out in Ref. [15], a positive effective range can only be described by this theory if $\sigma = -1$. In this case the free theory describes an atom and a ghost field. We will employ the Lagrangian (1) and will expand all elements of all Feynman graphs in powers of r_0 . The SREFT Lagrangian is then equivalent, order-by-order in the r_0 expansion, to the SREFT Lagrangian with an atom field alone, as presented in, e.g., Refs. [10, 12].

The Feynman rules are derived from Eq. (1) and the atom propagator in momentum space is

$$iS(p_0, p) = \frac{i}{p_0 - \frac{p^2}{2m} + i\epsilon}, \quad (2)$$

where p_0 is the energy and $p = |\mathbf{p}|$. The large scattering length leads to large loop effects, and the EFT power counting requires therefore that the two-body interaction is iterated to all orders (Fig.1). The resulting dressed dimer propagator is

$$i\mathcal{D}(p_0, p) = \frac{-i}{p_0 - \frac{p^2}{4m} - \Delta + \frac{mg^2}{4\pi} \sqrt{-mp_0 + \frac{p^2}{4} - i\epsilon} + i\epsilon}. \quad (3)$$

If the scattering length a is positive, the two-body system will display a bound state (*shallow dimer*). Equation (3) therefore has to have a pole at the on-shell four-momentum $p_0 =$

$\frac{p^2}{4m} - \frac{\gamma^2}{m}$, where $-\frac{\gamma^2}{m}$ is the binding energy of the shallow dimer. We can rewrite this condition and obtain

$$-\gamma^2 - m\Delta + \frac{m^2 g^2}{4\pi} \gamma = 0, \quad (4)$$

which has the solution

$$\gamma = \frac{m^2 g^2}{8\pi} \left(1 - \sqrt{1 - \frac{64\pi^2 \Delta}{m^2 g^2}} \right). \quad (5)$$

We can relate the coupling constants g and Δ to scattering length a and effective range r_0 by using the S-wave effective range expansion

$$-\frac{1}{a} = -\gamma + \frac{1}{2} r_0 \gamma^2 \quad (6)$$

which leads to $a = \frac{mg^2}{4\pi} \frac{1}{\Delta}$ and $r_0 = \frac{8\pi}{m^2 g^2}$. Note that $\sigma = -1$ was used in Eq. (1) to derive these results. In terms of these quantities, the wave-function renormalization factor Z for this bound state is:

$$\frac{1}{Z} = i \frac{\partial}{\partial p_0} (i\mathcal{D}(p))^{-1} \Big|_{p_0 = \frac{p^2}{4m} - \frac{\gamma^2}{m}} = \frac{m^2 g^2}{8\pi \gamma} (1 - r_0 \gamma). \quad (7)$$

Thus, the dressed dimer propagator can be reexpressed as

$$i\mathcal{D}(p_0, p) = \frac{-i4\pi/mg^2}{-\gamma + \frac{1}{2}r_0(\gamma^2 + mp_0 - p^2/4) + \sqrt{-mp_0 + p^2/4 - i\epsilon + i\epsilon}}. \quad (8)$$

Two-body scattering phaseshifts for relative momentum k can be obtained from the propagator $\mathcal{D}(p_0, p)$ by evaluating it at the on-shell point of two atoms scattering with center-of-mass momentum $\mathbf{p} = 0$ and $E = k^2/m$, and multiplying it by $-ig^2$. This yields a two-body amplitude:

$$\frac{4\pi}{m} \frac{1}{\gamma - \frac{1}{2}r_0(\gamma^2 + k^2) + ik}, \quad (9)$$

i.e. one in conformity with the effective-range expansion around the two-body bound-state pole.

However, the propagator in Eq. (8) cannot be directly employed in an integral equation for three-body physics, since it contains a spurious pole. This deep bound state (pole at momentum $\sim 1/r_0$) arises since we have chosen to work with a ghost field that leads to unphysical features in the theory, such as negative-norm states and/or violations of unitarity. However, when we expand the propagator in powers of γr_0 , the deep pole does not appear at any finite order:

$$i\mathcal{D}(p_0, p) = \sum_n \frac{-i4\pi/mg^2}{-\gamma + \sqrt{-mp_0 + p^2 - i\epsilon + i\epsilon}} \left(\frac{r_0}{2}\right)^n \left(\gamma + \sqrt{-mp_0 + p^2/4}\right)^n. \quad (10)$$



FIG. 1: The series that is summed to obtain the dressed dimer propagator, leading to Eq. (3).

The leading-order (LO) dimer propagator is therefore given by

$$i\mathcal{D}^{(0)}(p_0, p) = \frac{-i4\pi/mg^2}{-\gamma + \sqrt{-mp_0 + p^2 - i\epsilon + i\epsilon}}, \quad (11)$$

and the next-to-leading order $\mathcal{O}(\gamma r_0)$ correction is

$$i\mathcal{D}^{(1)}(p_0, p) = -i \frac{4\pi}{mg^2} \times \frac{r_0}{2} \frac{\gamma + \sqrt{-mp_0 + p^2/4}}{-\gamma + \sqrt{-mp_0 + p^2/4}}. \quad (12)$$

III. THREE-BODY AMPLITUDES

The calculation of three-body observables requires the solution of an integral equation which we will call the modified Skorniakov-Ter-Martirosian equation. It is the Faddeev equation for non-relativistic particles interacting through two-body and three-body zero-range interactions. We will show this equation below. Details of its derivation can be found in Refs. [3, 4]. A three-body interaction is included there, to ensure cutoff-independent results. The running of the associated coupling constant (h) displays a limit cycle.

Our analysis concerns the corrections to the modified STM equation and is based on rewriting all involved quantities in the form

$$\begin{aligned} \mathcal{D}(p) &= \mathcal{D}^{(0)}(p) + \mathcal{D}^{(1)}(p) + \dots \\ t(q, p) &= t^{(0)}(q, p) + t^{(1)}(q, p) + \dots \\ H(\Lambda) &= H_0(\Lambda) + H_1(\gamma, \Lambda) + \dots, \end{aligned} \quad (13)$$

where $H(\Lambda) = \Lambda^2 h / 2mg^2$, and each quantity in Eq. (13) is expanded in powers of $k r_0$ and γr_0 . Hence all quantities in the calculations that follow are computed up to next-to-leading order in the ℓ/a expansion. Since $\gamma, k \sim 1/a$ and we assume $r_0 \sim \ell$, this implies that our goal in this work is to compute $t^{(1)}$ and associated NLO parts of physical observables in this expansion. The t -matrix obtained in this way is then related to the renormalized amplitude

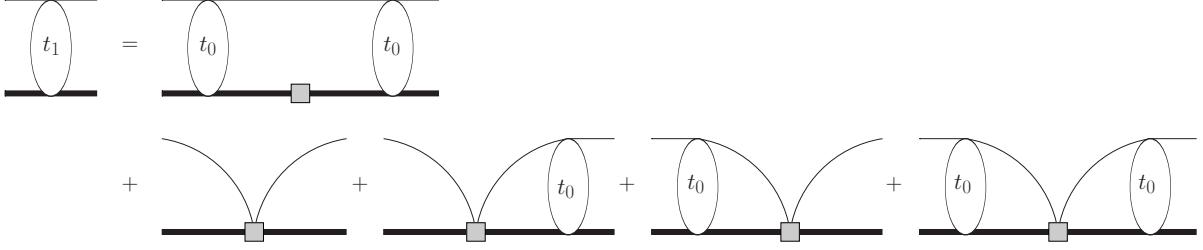


FIG. 2: The diagrams for the next-to-leading order t-matrix. Propagators and vertices with gray squares denote NLO corrections.

for s-wave atom-dimer scattering at relative momentum k , $T(k)$, via:

$$T(k) = \sqrt{Z}(t_0(k, k; E) + t_1(k, k; E) + \dots)\sqrt{Z}, \quad (14)$$

where, for elastic atom-dimer scattering, the magnitude of the relative incoming momentum $|\mathbf{k}|$ equals the relative outgoing momentum $|\mathbf{p}|$ and the three-body energy, E , is given by:

$$E = \frac{3k^2}{4m} - \frac{\gamma^2}{m}. \quad (15)$$

In Eq. (14), Z is the wave-function renormalization factor given in Eq. (7). We also expand this Z -factor in powers of γr_0 :

$$Z_0 = \frac{8\pi\gamma}{m^2g^2}, \quad Z_1 = \frac{8\pi\gamma^2r_0}{m^2g^2}, \quad (16)$$

and so on, thereby generating an expansion for $T(k)$ analogous to those listed in Eq. (13).

The leading-order three-body amplitude, t_0 , is computed by iterating the two- and three-body interactions of Eq. (1) to all orders via the integral equation [4]

$$\tilde{t}_0(q, p; E) = M(q, p; E) + \frac{2}{\pi} \int_0^\Lambda dq' \frac{q'^2}{-\gamma + \sqrt{3q'^3/4 - mE - i\epsilon}} M(q', p; E) \tilde{t}_0(q, q'; E), \quad (17)$$

where

$$M(q, p; E) = \frac{1}{qp} \log \left(\frac{q^2 + p^2 + qp - mE}{q^2 + p^2 - qp - mE} \right) + \frac{2H_0(\Lambda)}{\Lambda^2}. \quad (18)$$

Note that we have rescaled the t-matrix in Eq. (17) $t_0(q, p; E) = mg^2\tilde{t}_0(q, p; E)$ such that it depends only on physical quantities. The integral equation without the three-body force was first derived by Skorniakov and Ter-Martirosian and corresponds to three particles interacting through zero-range two-body interactions [22].

The LO three-body force, $H_0(\Lambda)$ is fixed by fitting it to one three-body observable. A combination of analytical arguments and numerical studies then show that $H_0(\Lambda)$ varies with Λ as:

$$H_0(\Lambda) = c \frac{\sin(s_0 \ln(\Lambda/\bar{\Lambda}) + \arctan(s_0))}{\sin(s_0 \ln(\Lambda/\bar{\Lambda}) - \arctan(s_0))}, \quad (19)$$

The constant c is $\mathcal{O}(1)$ and depends on details of the regularization of the modified STM equation. For the regulator employed in Eq. (17) we confirm the value $c = 0.879$ determined numerically in Ref. [21].

We calculate corrections to the amplitude obtained from the LO modified STM equation, \tilde{t}_0 , by considering diagrams with a single insertion of the NLO dimer propagator. It was shown by Hammer and Mehen [5] that such a perturbative inclusion of effective range corrections also requires the insertion of a subleading, energy-independent, three-body force. In Fig. 2 we display the diagrams that have to be evaluated. The application of the Feynman rules gives, for the first-order correction to the amplitude

$$\begin{aligned} it^{(1)}(\mathbf{q}, \mathbf{p}; E) &= \int \frac{d^4 q'}{(2\pi)^4} iS(E - q'_0, q') i\mathcal{D}^{(1)}(q'_0, q') \\ &\quad \times it^{(0)}(\mathbf{q}, \mathbf{q}', q'_0 - E + \frac{q'^2}{2m}) it^{(0)}(\mathbf{q}', \mathbf{p}, E - \frac{q'^2}{2m} - q'_0) \\ &\quad + i \frac{2mg^2 H_1(\gamma, \Lambda)}{\Lambda^2} \\ &\quad \times \left[1 + \int \frac{d^4 q'}{(2\pi)^4} i\mathcal{D}^{(0)}(q'_0, q') iS(E - q'_0, q') it_0(\mathbf{q}, \mathbf{q}', q'_0 - E + \frac{q'^2}{2m}) \right] \\ &\quad \times \left[1 + \int \frac{d^4 q'}{(2\pi)^4} i\mathcal{D}^{(0)}(q'_0, q') iS(E - q'_0, q') it_0(\mathbf{q}', \mathbf{p}, E - \frac{q'^2}{2m} - q'_0) \right]. \end{aligned} \quad (20)$$

The complete NLO correction to the S-wave projection of the t-matrix is therefore

$$\begin{aligned} \tilde{t}_1(q, p; E) &= \frac{1}{\pi} \int_0^\Lambda dq' q'^2 \frac{\gamma + \sqrt{3q'^2/4 - mE}}{-\gamma + \sqrt{3q'^2/4 - mE} - i\varepsilon} \tilde{t}_0(q, q'; E) \tilde{t}_0(q', p; E) \\ &\quad + \frac{2\tilde{H}_1(\gamma, \Lambda)}{\Lambda^2} \left[1 + \frac{2}{\pi} \int_0^\Lambda dq' \frac{q'^2}{-\gamma + \sqrt{3q'^2/4 - mE} - i\varepsilon} \tilde{t}_0(q, q'; E) \right] \\ &\quad \times \left[1 + \frac{2}{\pi} \int_0^\Lambda dq' \frac{q'^2}{-\gamma + \sqrt{3q'^2/4 - mE} - i\varepsilon} \tilde{t}_0(q', p; E) \right], \end{aligned} \quad (21)$$

where \tilde{t}_1 and \tilde{H}_1 are defined via $t_1(q, p; E) \equiv r_0 m g^2 \tilde{t}_1(q, p; E)$, and $H_1 \equiv r_0 \tilde{H}_1$.

The expression above is similar to the one obtained by Hammer and Mehen in Ref. [5].

However, in their work one contribution from the contour integration in Eq. (20) was erroneously omitted. In that approximation the first term in Eq. (21) becomes:

$$\frac{1}{\pi} \int_0^\Lambda dq' q'^2 \frac{2\gamma}{-\gamma + \sqrt{3q'^2/4 - mE} - i\epsilon} \tilde{t}_0(q, q'; E) \tilde{t}_0(q', p; E). \quad (22)$$

As will become clear below, this omission leads to the conclusion that only one counterterm is required to renormalize the three-body problem in SREFT at NLO. While this works in practice for fixed- a observables, such as the neutron-deuteron phase shifts computed in Ref. [5], it produces incorrect results if experiments in which a varies, like those examining loss features in gases of cold atoms, are analyzed.

\tilde{t}_0 , \tilde{t}_1 , etc. are generally complex when scattering states are considered, albeit real when the bound-state problem is considered. It is therefore convenient to introduce the real K-matrix, which contains the same information as the t-matrix but is easier to calculate. The LO half-on-shell K-matrix obeys an STM equation in which the $i\epsilon$ prescription is replaced by a principal-value integration (indicated by \mathcal{P})

$$\tilde{K}_0(k, p; E) = M(k, p; E) + \frac{8}{3\pi} \mathcal{P} \int_0^\Lambda dq' \frac{q'^2(\gamma + \sqrt{3q'^3/4 - mE})}{q'^2 - k^2} M(q', p; E) \tilde{K}_0(k, q'; E). \quad (23)$$

The half-on-shell t-matrix at LO is related to the K-matrix via

$$\tilde{t}_0(k, p; E) = \frac{\tilde{K}_0(k, p; E)}{1 - i\frac{8\gamma k}{3} \tilde{K}_0(k, k; E)}. \quad (24)$$

The fully-off-shell t-matrix at leading order is also related to the K-matrix through a similar transformation

$$\tilde{t}_0(q, p; E) = \tilde{K}_0(q, p; E) + i\frac{8\gamma k}{3} \tilde{K}_0(k, p; E) \tilde{t}_0(q, k; E). \quad (25)$$

This allows us to write the fully-off-shell K-matrix as

$$\tilde{K}_0(q, p; E) = M(q, p; E) + \frac{8}{3\pi} \mathcal{P} \int_0^\Lambda dq' \frac{q'^2(\gamma + \sqrt{3q'^3/4 - mE})}{q'^2 - k^2} M(q', p; E) \tilde{K}_0(q, q'; E), \quad (26)$$

with E and k related as in Eq. (15). The half-on-shell NLO K-matrix can then be expressed in terms of the half-on-shell LO and NLO t-matrix and the on-shell LO t-matrix, LO K-Matrix and NLO K-matrix

$$\tilde{K}_1(k, p; E) = \frac{\tilde{t}_1(k, p; E)}{1 + i\frac{8\gamma k}{3} \tilde{t}_0(k, k; E)} - i\frac{8\gamma k}{3} \tilde{t}_0(k, p; E) \left[\tilde{K}_1(k, k; E) + \gamma \tilde{K}_0(k, k; E) \right], \quad (27)$$

or vice versa

$$\tilde{t}_1(k, p; E) = \frac{\tilde{K}_1(k, p; E)}{1 - i\frac{8\gamma k}{3}\tilde{K}_0(k, k; E)} + \frac{i\frac{8\gamma k}{3}\tilde{K}_0(k, p; E) \left[\tilde{K}_1(k, k; E) + \gamma\tilde{K}_0(k, k; E) \right]}{\left[1 - i\frac{8\gamma k}{3}\tilde{K}_0(k, k; E) \right]^2}. \quad (28)$$

At next-to-leading order, the half-on-shell K-matrix is then given by the following principal-value integral:

$$\begin{aligned} \tilde{K}_1(k, p; E) = & \frac{1}{\pi} \mathcal{P} \int_0^\Lambda dq' q'^2 \frac{\gamma + \sqrt{3q'^2/4 - mE}}{-\gamma + \sqrt{3q'^2/4 - mE}} \tilde{K}_0(k, q'; E) \tilde{K}_0(p, q'; E) \\ & + \frac{2\tilde{H}_1(\gamma, \Lambda)}{\Lambda^2} \left[1 + \frac{2}{\pi} \mathcal{P} \int_0^\Lambda dq' \frac{q'^2}{-\gamma + \sqrt{3q'^2/4 - mE}} \tilde{K}_0(k, q'; E) \right] \\ & \times \left[1 + \frac{2}{\pi} \mathcal{P} \int_0^\Lambda dq' \frac{q'^2}{-\gamma + \sqrt{3q'^2/4 - mE}} \tilde{K}_0(p, q'; E) \right]. \quad (29) \end{aligned}$$

IV. THREE-BODY OBSERVABLES AT NLO

In this section we will discuss how different observables are calculated at NLO in our perturbative approach. We will consider not only obvious observables, such as phaseshifts and three-body binding energies, but also observables typically measured in experiments with ultracold atoms. We follow the strategy outlined above and calculate all quantities as a series in powers of γr_0 and/or $k r_0$. The leading order in this series is then the universal result, and the NLO pieces we will derive here encode the first corrections “beyond universality”.

A. Phaseshifts

The amplitude $T(k)$ for atom-dimer scattering is related to the atom-dimer S-wave phase-shift through

$$T(k) = \frac{3\pi}{m} \frac{1}{k \cot \delta(k) - ik}. \quad (30)$$

The scattering amplitude $T(k)$ in Eq. (30) can also be expanded in powers of γr_0

$$\begin{aligned} T(k) &= \frac{3\pi}{m} \frac{1}{k \cot \delta_0 + r_0 [k \cot \delta]_1 + \dots - ik} \\ &= \frac{3\pi}{m} \left[\frac{1}{k \cot \delta_0 - ik} - r_0 \frac{[k \cot \delta]_1}{(k \cot \delta_0 - ik)^2} + \dots \right] \\ &= T_0(k) + T_1(k) + \dots, \quad (31) \end{aligned}$$

where the dots refer to corrections beyond NLO. Here $k \cot \delta$ is expanded as

$$k \cot \delta = k \cot \delta_0 + r_0 [k \cot \delta]_1 + \dots, \quad (32)$$

where the $[\]_1$ indicates the part of $k \cot \delta$ that is the coefficient of the order r_0 term in the expansion in powers of r_0 . At leading order we recover the familiar relation between phaseshifts and K-matrix

$$k \cot \delta_0 = \frac{3}{8\gamma} \tilde{K}_0^{-1}(k, k; E), \quad (33)$$

but our expansion also leads to a relation for the NLO part, that stems from Eqs. (31) and (28):

$$[k \cot \delta]_1 = -\frac{3}{8\gamma} \tilde{K}_0^{-1}(k, k; E) \left(\gamma + \tilde{K}_1(k, k; E) / \tilde{K}_0(k, k; E) \right). \quad (34)$$

As long as $k \cot \delta_0$ is not large this will yield a correction of relative size γr_0 to the leading part of $k \cot \delta$.

B. Bound States

The t-matrix is real for energies below the scattering threshold. The NLO correction to the leading order t-matrix is then given by

$$\begin{aligned} \tilde{t}_1(q, p; E) = & \frac{1}{\pi} \int_0^\Lambda dq' q'^2 \frac{\gamma + \sqrt{3q'^2/4 - mE}}{-\gamma + \sqrt{3q'^2/4 - mE}} \tilde{t}_0(q, q'; E) \tilde{t}_0(p, q'; E) \\ & + \frac{2\tilde{H}_1(\gamma, \Lambda)}{\Lambda^2} \left[1 + \frac{2}{\pi} \int_0^\Lambda dq' \frac{q'^2}{-\gamma + \sqrt{3q'^2/4 - mE}} \tilde{t}_0(q, q'; E) \right] \\ & \times \left[1 + \frac{2}{\pi} \int_0^\Lambda dq' \frac{q'^2}{-\gamma + \sqrt{3q'^2/4 - mE}} \tilde{t}_0(p, q'; E) \right], \quad (35) \end{aligned}$$

where we have explicitly dropped the $i\epsilon$ prescription. The full t-matrix has a pole at $E = B$ if a three-body bound state exists with this energy. At leading order this implies:

$$\tilde{t}_0(q, p; E) = \frac{\tilde{Z}_0(q, p)}{E - B_0} + \mathcal{R}_0(q, p; E) \quad (36)$$

where the function \mathcal{R}_0 is a regular part. The residue \tilde{Z}_0 depends on the incoming and outgoing momenta q and p , but not on the three-body energy E . Although, in general, more than one bound state exists for the systems under consideration here, the decomposition (36) is the appropriate one if we are focusing on the NLO shift for a particular bound state. The

fact that LO bound-state energies are separated by a factor as large as 515 allows us to employ the decomposition (36) for these purposes.

When considering the NLO correction, we must account for both the pole's position (i.e. the three-body binding energy) and the residue being shifted by an amount proportional to r_0 . Therefore we have

$$\begin{aligned} \tilde{t}_0 + r_0 \tilde{t}_1 &= \frac{\tilde{Z}_0 + \tilde{Z}_1}{E - B_0 - B_1} + \mathcal{R}_0 + \mathcal{R}_1 \\ &= \frac{\tilde{Z}_0}{E - B_0} + \frac{\tilde{Z}_0 B_1}{(E - B_0)^2} + \frac{\tilde{Z}_1}{E - B_0} + \mathcal{R}_0 + \mathcal{R}_1, \end{aligned} \quad (37)$$

where, as usual, the subscript 1 indicates the parts which are first order in r_0 . In particular, Eqs. (37) and (36) imply that the first-order part of \tilde{t} , $r_0 \tilde{t}_1$, has a pole of order two at $E = B_0$:

$$r_0 \tilde{t}_1(q, p; E) = \frac{\tilde{Z}_0(q, p) B_1}{(E - B_0)^2} + \frac{\tilde{Z}_1}{E - B_0} + \mathcal{R}_1(q, p; E). \quad (38)$$

The residue of this double pole is then related to the shift in the three-body binding energy that is linear in the effective range:

$$B_1 = r_0 \frac{\lim_{E \rightarrow B_0} (E - B_0)^2 \tilde{t}_1(q, p; E)}{\tilde{Z}_0(q, p)}. \quad (39)$$

Equation (39) seems to indicate that the incoming and outgoing momenta, q and p , affect the three-body binding energy shift B_1 . However, we would expect that the binding energy is independent of the incoming and outgoing momenta. This apparent contradiction can be avoided if $\tilde{Z}_0(q, p)$ is separable with respect to q and p . Therefore, the residue function is defined as

$$\tilde{Z}_0(q, p) = \Gamma(q)\Gamma(p). \quad (40)$$

By substituting Eqs. (40) and (36) into Eq. (17) and taking the residue at $E = B_0$ we find

$$\Gamma(q) = \frac{2}{\pi} \int_0^\Lambda dq' M(q, q'; E) \frac{q'^2}{-\gamma + \sqrt{3q'^2/4 - mE}} \Gamma(q'). \quad (41)$$

The function $\Gamma(q)$ is thus a solution to a homogeneous integral equation, and the overall normalization is not immediately determined. We fix this normalization by the condition:

$$\Gamma^2(q) = \lim_{E \rightarrow B_0} (E - B_0) \tilde{t}_0(q, q; E). \quad (42)$$

With $\Gamma(q)$ in hand, we can insert Eq. (40) into Eq. (35), and multiply by $(E - B_0)^2$ and take the limit as $E \rightarrow B_0$. This yields a result for B_1 that is independent of q and p :

$$B_1 = \frac{r_0}{\pi} \int_0^\Lambda dq q^2 \frac{\gamma + \sqrt{3q^2/4 - mB_0}}{-\gamma + \sqrt{3q^2/4 - mB_0}} \Gamma^2(q) + \frac{8\tilde{H}_1(\Lambda)r_0}{(\pi\Lambda)^2} \left[\int_0^\Lambda dq \frac{q^2}{-\gamma + \sqrt{3q^2/4 - mB_0}} \Gamma(q) \right]^2. \quad (43)$$

And indeed, in numerical calculations, Eqs. (39) and (43) prove to be equivalent. B_1 can be obtained from Eq. (39) if desired, and the result found in that way is independent of q and p .

C. Three-Body Recombination

Three-body recombination is a collision process in which three free atoms combine into a dimer and an atom. The atoms can either recombine into deeply bound two-body states (*deep dimers*) whose properties cannot be described by the SREFT (but see Ref. [13] for a discussion on how the effects of these deep states can be included in the theory), or, provided the scattering length a is positive, into the two-body bound state which is explicitly included in SREFT. The energy that is released when the two-atom bound state forms is converted into kinetic energy and atom and diatom are lost from the trap. The loss rate of atoms in a cold atomic gas due to three-body recombination into the shallow dimer is determined by the scattering amplitude for the reaction $A + A + A \rightarrow A + D$, as we shall now show. The scattering-length dependence of the loss rate therefore provides an experimental signature of Efimov physics in trapped systems of ultracold atoms.

The atom loss rate is expressed as

$$\frac{dn}{dt} = -3 \frac{n^3}{3!} W_{fi}, \quad (44)$$

where n is the number density of free atoms. (The factor of 3 arises due to the loss of three atoms in each recombination event.) According to Fermi's golden rule,

$$W_{fi} = 2\pi |T(p_f)|^2 \frac{d\nu_f}{dE_f}, \quad (45)$$

where T is the amplitude for three-atom recombination: $A + A + A \rightarrow A + D$, and the density of atom-dimer states $d\nu_f$ is

$$d\nu_f = \frac{d^3 p_f}{(2\pi)^3}. \quad (46)$$

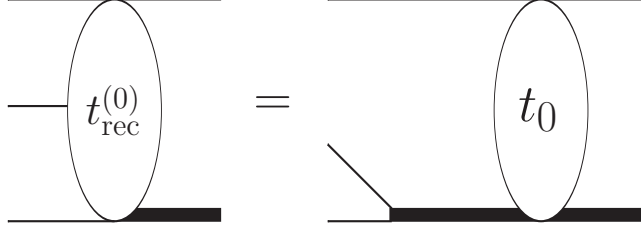


FIG. 3: Three-body recombination at leading order

The kinetic energy at a momentum p_f in the atom-dimer system is

$$E_f = \frac{p_f^2}{2m} + \frac{p_f^2}{4m} = \frac{3p_f^2}{4m}, \quad (47)$$

and so the transition rate becomes

$$W_{fi} = \frac{2m}{3\pi} p_f |t_{\text{rec}}(p_f)|^2. \quad (48)$$

The recombination rate α is conventionally defined as

$$\frac{dn}{dt} = -3\alpha n^3, \quad (49)$$

and so

$$\alpha = \frac{m}{9\pi} p_f |t_{\text{rec}}(p_f)|^2. \quad (50)$$

At zero temperature three-body recombination takes place at the three-atom threshold and the value of the relative momentum p_f in the atom-dimer system is therefore $2\gamma/\sqrt{3}$.

The $A + A + A \rightarrow A + D$ amplitude at leading order in Fig. 3 is related to the half-on-shell atom-dimer scattering t-matrix by

$$\begin{aligned} t_{\text{rec}}^{(0)}(p_f) &= 3 \cdot (-i\sqrt{2}g) \cdot i\mathcal{D}^{(0)}(0, 0) \cdot \sqrt{Z_0} t_0(0, p_f; 0) \\ &= \frac{48\pi^{\frac{3}{2}}}{m\sqrt{\gamma}} \tilde{t}_0 \left(0, \frac{2\gamma}{\sqrt{3}}; 0 \right), \end{aligned} \quad (51)$$

which, combined with Eq. (50), determines the leading-order recombination rate as:

$$\alpha_0 = \frac{512\pi^2}{\sqrt{3}m} \left| \tilde{t}_0 \left(0, \frac{2\gamma}{\sqrt{3}}; 0 \right) \right|^2. \quad (52)$$

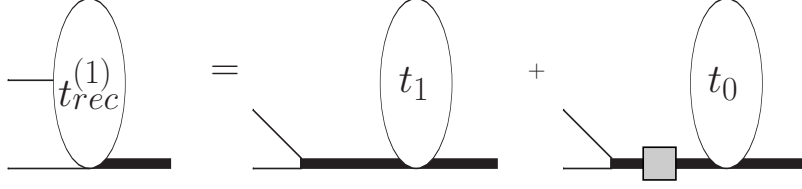


FIG. 4: Three-body recombination at next-to-leading order

Upon introducing the effective-range correction, we obtain the sum of the leading-order and next-to-leading-order $A + A + A \rightarrow A + D$ amplitude (Fig.4). This is expressed by

$$\begin{aligned}
t_{\text{rec}}^{(0)}(p_f) + t_{\text{rec}}^{(1)}(p_f) &= 3 \cdot (-i\sqrt{2}g)\sqrt{Z_0 + Z_1} \cdot [i\mathcal{D}^{(0)}(0,0)t_0 + i\mathcal{D}^{(1)}(0,0)t_0 + i\mathcal{D}^{(0)}(0,0)t_1] \\
&= t_{\text{rec}}^{(0)} + 3\sqrt{2}g \left[\sqrt{Z_0} \mathcal{D}^{(1)}(0,0)t_0 + \frac{Z_1}{2\sqrt{Z_0}} \mathcal{D}^{(0)}(0,0)t_0 + \sqrt{Z_0} \mathcal{D}^{(0)}(0,0)t_1 \right] + \dots, \\
&= t_{\text{rec}}^{(0)} + \frac{48\pi^{3/2}}{m\gamma^{1/2}} [\gamma r_0 \tilde{t}_0 + r_0 \tilde{t}_1] \\
\Rightarrow t_{\text{rec}}^{(1)}(p_f) &= \frac{48\pi^{3/2}}{m\gamma^{1/2}} \left(\gamma r_0 \tilde{t}_0(0, 2\gamma/\sqrt{3}; 0) + r_0 \tilde{t}_1(0, 2\gamma/\sqrt{3}; 0) \right). \tag{53}
\end{aligned}$$

Therefore, the recombination rate is given at NLO by:

$$\alpha_0 + \alpha_1 = \frac{512\pi^2}{\sqrt{3}m} \left| \left(\tilde{t}_0(0, \frac{2\gamma}{\sqrt{3}}; 0) + \gamma r_0 \tilde{t}_0(0, \frac{2\gamma}{\sqrt{3}}; 0) + r_0 \tilde{t}_1(0, \frac{2\gamma}{\sqrt{3}}; 0) \right) \right|^2. \tag{54}$$

1. Recombination minimum

At leading order the recombination rate α is related to \tilde{K}_0 by

$$\alpha_0 = \frac{512\pi^2}{\sqrt{3}m} \frac{\tilde{K}_0^2(0, \frac{2\gamma}{\sqrt{3}}; 0)}{\left| 1 - i\frac{16\gamma^2}{3\sqrt{3}} \tilde{K}_0(\frac{2\gamma}{\sqrt{3}}, \frac{2\gamma}{\sqrt{3}}; 0) \right|^2}. \tag{55}$$

Therefore, the recombination minimum is determined by the condition $\tilde{K}_0(0, \frac{2\gamma_0}{\sqrt{3}}; 0) = 0$, which leads to $\tilde{t}_0(0, \frac{2\gamma_0}{\sqrt{3}}; 0) = 0$.

Because $\alpha_0 = 0$ at the minimum, the NLO recombination rate in Eq. (54) becomes $\mathcal{O}(r_0^2)$ in the vicinity of the leading-order minimum. This means that in what follows we cannot neglect terms $\sim r_0^2$, which complete the square and guarantee that $\alpha > 0$.

In order to calculate the NLO correction to the recombination minimum, we evaluate α_1 from Eq. (54) at $\gamma = \gamma_0 + \Delta\gamma_0$, and expand it in powers of r_0 . First, we expand the

scattering amplitude before we square it:

$$\begin{aligned} & \left[(1 + \gamma r_0) \tilde{t}_0(0, \frac{2\gamma}{\sqrt{3}}; 0) + r_0 \tilde{t}_1(0, \frac{2\gamma}{\sqrt{3}}; 0) \right] \Big|_{\gamma=\gamma_0+\Delta\gamma} \\ &= \frac{d}{d\gamma} \tilde{t}_0(0, \frac{2\gamma}{\sqrt{3}}; 0) \Big|_{\gamma=\gamma_0} \Delta\gamma + r_0 \tilde{t}_1(0, \frac{2\gamma_0}{\sqrt{3}}; 0) + \mathcal{O}(r_0^2), \end{aligned} \quad (56)$$

where $\Delta\gamma$ is linear in r_0 , and we used the fact that $\tilde{t}_0(0, \frac{2\gamma_0}{\sqrt{3}}; 0) = 0$.

If we square the amplitude in Eq. (56), we can calculate α_1 at γ near γ_0 as

$$\alpha_1 = \frac{512\pi^2}{\sqrt{3}m} \left| \frac{d}{d\gamma} \tilde{t}_0(0, \frac{2\gamma}{\sqrt{3}}; 0) \Big|_{\gamma=\gamma_0} \Delta\gamma + r_0 \tilde{t}_1(0, \frac{2\gamma_0}{\sqrt{3}}; 0) \right|^2 + \mathcal{O}(r_0^3), \quad (57)$$

where we used the fact that $\alpha_0 = 0$ at $\gamma = \gamma_0$. The leading term here is quadratic in r_0 and purely determined by up-to-NLO scattering amplitudes. Higher-order corrections to the scattering amplitude only start to affect α at order r_0^3 . In other words, even though the NLO α near γ_0 is in the order of r_0^2 , it is purely determined by LO and NLO t-matrices.

From Eq. (25) and Eq. (28), we derive

$$\frac{d}{d\gamma} \tilde{t}_0(0, \frac{2\gamma}{\sqrt{3}}; 0) \Big|_{\gamma=\gamma_0} = \frac{1}{1 - i \frac{16\gamma_0^2}{3\sqrt{3}} \tilde{K}_0(\frac{2\gamma_0}{\sqrt{3}}, \frac{2\gamma_0}{\sqrt{3}}; 0)} \cdot \frac{d}{d\gamma} \tilde{K}_0(0, \frac{2\gamma}{\sqrt{3}}; 0) \Big|_{\gamma=\gamma_0}, \quad (58)$$

and

$$\tilde{t}_1(0, \frac{2\gamma_0}{\sqrt{3}}; 0) = \frac{\tilde{K}_1(0, \frac{2\gamma_0}{\sqrt{3}}; 0)}{1 - i \frac{16\gamma_0^2}{3\sqrt{3}} \tilde{K}_0(\frac{2\gamma_0}{\sqrt{3}}, \frac{2\gamma_0}{\sqrt{3}}; 0)}, \quad (59)$$

where we again applied $\tilde{K}_0(0, \frac{2\gamma_0}{\sqrt{3}}; 0) = 0$.

Therefore, α_1 near γ_0 is

$$\alpha_1 = \frac{512\pi^2}{\sqrt{3}m} \frac{\left[\frac{d}{d\gamma} \tilde{K}_0(0, \frac{2\gamma}{\sqrt{3}}; 0) \Big|_{\gamma=\gamma_0} \Delta\gamma + r_0 \tilde{K}_1(0, \frac{2\gamma_0}{\sqrt{3}}; 0) \right]^2}{\left| 1 - i \frac{16\gamma_0^2}{3\sqrt{3}} \tilde{K}_0(\frac{2\gamma_0}{\sqrt{3}}, \frac{2\gamma_0}{\sqrt{3}}; 0) \right|^2} \quad (60)$$

The next-to-leading-order recombination minimum $\alpha_1 = 0$ is thus determined by

$$\frac{d}{d\gamma} \tilde{K}_0 \left(0, \frac{2\gamma}{\sqrt{3}}; 0 \right) \Big|_{\gamma=\gamma_0} \Delta\gamma_0 + r_0 \tilde{K}_1 \left(0, \frac{2\gamma_0}{\sqrt{3}}; 0 \right) = 0, \quad (61)$$

which leads to an NLO shift in the position of the recombination minimum of:

$$\Delta\gamma_0 = -r_0 \frac{\tilde{K}_1(0, \frac{2\gamma_0}{\sqrt{3}}; 0)}{\frac{d}{d\gamma} \tilde{K}_0(0, \frac{2\gamma}{\sqrt{3}}; 0) \Big|_{\gamma=\gamma_0}}. \quad (62)$$

D. Atom-Dimer Resonance

The atom-dimer scattering length diverges for positive scattering lengths for which $B = -\gamma^2/m$. At this value of the scattering length, a three-body state lies exactly at the atom-diatom threshold. This feature shows up as resonant behavior in the atom-dimer relaxation rate, a process in which shallow dimers are transferred through collision processes into deep dimers. The two-body binding momenta for which these resonances occur are denoted (at LO) by γ_* . They thus obey the relation

$$B_0(\gamma_*) = -\frac{\gamma_*^2}{m}. \quad (63)$$

Discrete scale invariance in the leading-order bound-state spectrum implies that if γ_* is a solution of Eq. (63), then so are the quantities $e^{n\pi/s_0}\gamma_*$. The scale invariance is softly broken by r_0/a corrections. Here we will calculate the NLO corrections to these γ_* 's.

We will assume that the position of a particular resonance is shifted to $\gamma_* + \Delta\gamma_*$ at NLO. The three-body binding energy at the atom-dimer threshold must then obey up to terms of relative order $\mathcal{O}(\gamma_*^2 r_0^2)$:

$$B_0(\gamma_* + \Delta\gamma_*) + B_1(\gamma_* + \Delta\gamma_*) = -\frac{(\gamma_* + \Delta\gamma_*)^2}{m}. \quad (64)$$

We now expand both sides of (64) in powers of r_0 and retain only terms up to $\mathcal{O}(r_0)$:

$$B_0(\gamma_*) + \left. \frac{dB_0(\gamma)}{d\gamma} \right|_{\gamma=\gamma_*} \Delta\gamma_* + B_1(\gamma_*) = -\frac{\gamma_*^2}{m} - 2\frac{\gamma_* \Delta\gamma_*}{m}. \quad (65)$$

Using Eq. (63) we find a NLO correction to γ_*

$$\Delta\gamma_* = -\frac{mB_1(\gamma_*)}{2\gamma_* + m \left. \frac{dB_0(\gamma)}{d\gamma} \right|_{\gamma=\gamma_*}}. \quad (66)$$

We note that Eq. (43) implies that $\Delta\gamma_*$ is linear in r_0 .

However, calculating $\Delta\gamma_*$ according to Eq. (66) results in numerical difficulties, because $B_1(\gamma_*)$ and the denominator are both zero to within the numerical accuracy of our calculation.

The fact that the denominator should go to zero is clear from the expression given for $B_0(\gamma)$ in [13]:

$$\begin{aligned} \kappa &= -H \sin \xi \\ \gamma &= H \cos \xi \\ H &= (e^{-\pi/s_0})^{n-n_*} \kappa_* \exp[\Delta(\xi)/(2s_0)], \end{aligned} \quad (67)$$

where $\kappa = \sqrt{-mB_0}$. When γ is near γ_* the function $\Delta(\xi)$ can be expanded in power of $(-\pi/4 - \xi)^{1/2}$. For completeness we give the expression of Ref. [13], with the coefficients that were determined numerically there:

$$\xi \in \left[-\frac{3\pi}{8}, -\frac{\pi}{4} \right] : \Delta = 6.04 - 9.63\left(-\frac{\pi}{4} - \xi\right)^{1/2} + 3.10\left(-\frac{\pi}{4} - \xi\right), \quad (68)$$

where $\xi = -\pi/4$ corresponds to the three-body bound state crossing the atom-dimer threshold at $\gamma = \gamma_*$. We calculate $d\kappa/d\gamma$ from Eq. (67) and find that at $\xi = -\pi/4$,

$$\left. \frac{d\kappa}{d\gamma} \right|_{\gamma=\gamma_*} = \left. \frac{\frac{dH}{d\xi} - H}{\frac{dH}{d\xi} + H} \right|_{\xi=-\pi/4} = \left. \frac{\frac{d\Delta}{d\xi} - 2s_0}{\frac{d\Delta}{d\xi} + 2s_0} \right|_{\xi=-\pi/4} = 1, \quad (69)$$

since $\frac{d\Delta}{d\xi} \rightarrow \infty$ when $\xi \rightarrow -\pi/4$. $dB_0/d\gamma$ at the atom-dimer threshold is therefore

$$m \left. \frac{dB_0}{d\gamma} \right|_{\gamma=\gamma_*} = -2\kappa \left. \frac{d\kappa}{d\gamma} \right|_{\gamma=\gamma_*} = -2\gamma_*. \quad (70)$$

This indicates that the denominator in Eq. (66) indeed goes to zero at the point of interest, which causes an accuracy problem in numerically calculating $\Delta\gamma_*$ from the bound-state side.

We calculate therefore instead $\Delta\gamma_*$ from the scattering amplitude, i.e. evaluate the atom-dimer K-matrix as a function of γ along the threshold line $E = -\gamma^2$. The LO three-body scattering length $a_3^{(0)}$ is related to \tilde{K}_0 at this energy by

$$a_3^{(0)} = -\frac{8\gamma}{3} \tilde{K}_0(0, 0; -\gamma^2). \quad (71)$$

Now $a_3^{(0)} \rightarrow \infty$ at $\gamma = \gamma_*$, and so the on-shell \tilde{K}_0 has a pole of order one at $\gamma = \gamma_*$:

$$\tilde{K}_0(0, 0; -\gamma^2) = \frac{Z_0^{ad}(\gamma_*)}{\gamma - \gamma_*} + \mathcal{R}_0(\gamma). \quad (72)$$

Similarly the NLO shift of the position of the atom-dimer resonance $\Delta\gamma_*$, can be written as

$$\begin{aligned} \tilde{K}_0(0, 0; -\gamma^2) + \gamma r_0 \tilde{K}_0(0, 0; -\gamma^2) + r_0 \tilde{K}_1(0, 0; -\gamma^2) &= \frac{Z_0^{ad} + Z_1^{ad}}{\gamma - \gamma_* - \Delta\gamma_*} + \mathcal{R}_0(\gamma) + \mathcal{R}_1(\gamma) \\ &= \frac{Z_0^{ad}}{\gamma - \gamma_*} + \frac{Z_1^{ad}}{\gamma - \gamma_*} + \Delta\gamma_* \frac{Z_0^{ad}}{(\gamma - \gamma_*)^2} + \mathcal{R}_0(\gamma) + \mathcal{R}_1(\gamma). \end{aligned} \quad (73)$$

The shift $\Delta\gamma_*$ is therefore calculated as:

$$\Delta\gamma_* = r_0 \frac{\lim_{\gamma \rightarrow \gamma_*} (\gamma - \gamma_*)^2 \tilde{K}_1(0, 0; -\gamma^2)}{Z_0^{ad}(\gamma_*)}. \quad (74)$$

Our numerical calculation shows that both the numerator and the denominator in this form are finite, and so calculating $\Delta\gamma_*$ by evaluating the atom-dimer K-matrix at different γ 's along the threshold line is an accurate procedure.

However, we still have to show that Eqs. (66) and (74) are equivalent for calculating $\Delta\gamma_*$. The bound-state form of the leading-order atom-dimer amplitude near a bound state of energy $B_0(\gamma)$ (Eq. (36)) is:

$$\begin{aligned}\tilde{t}_0(0,0;-\gamma^2) &= \frac{m\tilde{Z}_0(0,0)}{-\gamma^2 - B_0(\gamma)} + \mathcal{R}_0 \\ &= -\frac{m\tilde{Z}_0(0,0)}{(\gamma - \gamma_*) \left[2\gamma_* + \frac{dB_0}{d\gamma} \Big|_{\gamma=\gamma_*} \right]} + (\text{regular}).\end{aligned}\quad (75)$$

This relates \tilde{Z}_0 in Eq. (36) to Z_0^{ad} in Eq. (72) as

$$\tilde{Z}_0(0,0) \Big|_{\gamma=\gamma_*} = - \left(2\gamma_* + \frac{dB_0}{d\gamma} \Big|_{\gamma=\gamma_*} \right) Z_0^{ad}(\gamma_*). \quad (76)$$

Similarly we expand (38) about γ_* and so relate $\tilde{Z}_0 B_1$ to the numerator in Eq. (74) as:

$$\tilde{Z}_0 B_1 \Big|_{\gamma=\gamma_*} = \left(2\gamma_* + \frac{dB_0}{d\gamma} \Big|_{\gamma=\gamma_*} \right)^2 r_0 \lim_{\gamma \rightarrow \gamma_*} (\gamma - \gamma_*)^2 \tilde{K}_1(0,0;-\gamma^2), \quad (77)$$

which explains why $B_1 \rightarrow 0$ as $\gamma \rightarrow \gamma_*$, and, moreover, shows that the coefficient of this zero is precisely what is needed to render the expressions obtained for $\Delta\gamma_*$ from the bound-state and scattering-state side equivalent.

E. Three-atom resonance

When a state in the three-body bound-state spectrum crosses the zero-energy threshold at negative scattering length, three free atoms can form a zero-energy trimer state. This phenomena is called a three-atom resonance, and results in a maximum in the three-atom recombination rate. It occurs at a value of γ denoted by γ_- . (Since $\gamma_- < 0$ this does not correspond to the binding momentum of a dimer, but it is still the inverse of the atom-atom scattering length where this feature occurs.) At leading order the condition for this three-atom resonance is $B_0(\gamma_-) = 0$. Furthermore, discrete scale invariance of the leading-order bound-state spectrum then results in values of γ_- being related by the universal scaling factor e^{π/s_0} . (Here and below γ_- denotes the leading-order position of the three-atom resonance.)

The NLO correction to γ_- is found at the NLO zero-energy threshold $(B_0 + B_1)(\gamma_- + \Delta\gamma_-) = 0$. We thus have:

$$B_0(\gamma_-) + \left. \frac{dB_0(\gamma)}{d\gamma} \right|_{\gamma=\gamma_-} \Delta\gamma_- + B_1(\gamma_-) = 0. \quad (78)$$

As $B_0(\gamma_-) = 0$ is given at LO, we find the NLO correction to γ_- ,

$$\Delta\gamma_- = -\frac{B_1(\gamma_-)}{\left. \frac{dB_0(\gamma)}{d\gamma} \right|_{\gamma=\gamma_-}}, \quad (79)$$

and so $\Delta\gamma_-$ is linear in r_0 . Our numerical studies show that neither the numerator nor the denominator in this equation are equal to zero at $\gamma = \gamma_-$. Our result is:

$$\left. \frac{dB_0(\gamma)}{d\gamma} \right|_{\gamma=\gamma_-} = -0.984\gamma_-, \quad (80)$$

where the coefficient is calculated with a numerical accuracy of about 10^{-3} . This is in contradiction to the form provided in Ref. [13], which predicts $\left. \frac{dB_0(\gamma)}{d\gamma} \right|_{\gamma=\gamma_-} = -2\gamma_-$. (See Appendix B.)

V. THE SUBLEADING THREE-BODY FORCE AT NLO

We will show in this section explicitly that the NLO counterterm contains a scattering-length-dependent piece that will require a second experimental datum for renormalization if scattering-length-dependent processes are considered. To do this we reconsider Eq. (43), the expression for the NLO shift to the binding energy:

$$B_1 = \frac{r_0}{\pi} \int^\Lambda dq q^2 \frac{\gamma + \sqrt{3q^2/4 - mB_0}}{-\gamma + \sqrt{3q^2/4 - mB_0}} \Gamma^2(q) + \frac{8\tilde{H}_1(\Lambda)r_0}{(\pi\Lambda)^2} \left[\int^\Lambda dq \frac{q^2}{-\gamma + \sqrt{3q^2/4 - mB_0}} \Gamma(q) \right]^2. \quad (81)$$

We will use the divergence structure of this observable to determine the behavior of $\tilde{H}_1(\Lambda)$ as a function of Λ , up to corrections $\sim 1/\Lambda$. The divergence structure of any other observable computed to NLO will be similar, and so it suffices to perform this calculation for B_1 . In particular, we will expand both the explicit integrals and the behavior of $\tilde{H}_1(\Lambda)$, in powers of Λ , and demand that the linear-in- Λ and $\log(\Lambda)$ divergences cancel.

In order to perform this analysis we need to know the large-momentum behavior of each term in Eq. (81). At large momenta q the function $\Gamma(q)$ is known in the form of an expansion

in powers of γ/q (see Appendix of Ref. [6] where we have corrected an error in the result for z_1):

$$\Gamma(q) \propto \frac{z_0}{q} + \frac{\gamma z_1}{q^2} + \dots, \quad (82)$$

with

$$z_0 = \sin\left(s_0 \ln \frac{q}{\Lambda}\right) \quad (83)$$

$$z_1 = \frac{2}{\sqrt{3}} |C_{-1}| \sin\left(s_0 \ln \frac{q}{\Lambda} + \arg C_{-1}\right) \quad (84)$$

where

$$C_{-1} = \frac{I(is_0 - 1)}{1 - I(is_0 - 1)} \quad (85)$$

and

$$I(s) = \frac{8 \sin(\frac{\pi s}{6})}{\sqrt{3} s \cos(\frac{\pi s}{2})}. \quad (86)$$

Inserting the asymptotic form of $\Gamma(q)$, (82), up to $\sim 1/q^2$, into Eq. (81), and evaluating the first integral shows that H_1 has to absorb both a linear divergence and a logarithmic divergence proportional to γ . In order to cancel these cutoff dependencies we will thus write \tilde{H}_1 as

$$\tilde{H}_1 = \Lambda h_{10}(\Lambda) + \gamma h_{11}(\Lambda). \quad (87)$$

Analytic expressions for both $h_{10}(\Lambda)$ and $h_{11}(\Lambda)$ can then be obtained by inserting the expansions (87) and (82) in Eq. (81), while also expanding all explicit functions of q in powers of γ/q . In this way we find:

$$\begin{aligned} \zeta &= \frac{1}{\pi} \int^\Lambda dq q^2 \left(1 + \frac{4\gamma}{\sqrt{3}q}\right) \frac{1}{q^2} \left(z_0^2 + \frac{2\gamma}{q} z_0 z_1\right) \\ &\quad + \frac{8\Lambda}{\pi^2 \Lambda^2} \left(h_{10} + \frac{\gamma}{\Lambda} h_{11}\right) \left[\frac{2}{\sqrt{3}} \int^\Lambda dq q \left(1 + \frac{2\gamma}{\sqrt{3}q}\right) \frac{1}{q} \left(z_0 + \frac{\gamma}{q} z_1\right)\right]^2 \\ &= \frac{1}{\pi} \int^\Lambda dq \left(z_0^2 + \frac{4\gamma}{\sqrt{3}q} z_0^2 + \frac{2\gamma}{q} z_0 z_1\right) \\ &\quad + \frac{8}{\pi^2 \Lambda} \left(h_{10} + \frac{\gamma}{\Lambda} h_{11}\right) \frac{4}{3} \left[\int^\Lambda dq \left(z_0 + \frac{2\gamma}{\sqrt{3}q} z_0 + \frac{\gamma}{q} z_1\right)\right]^2 + \dots, \end{aligned} \quad (88)$$

where ζ is finite, the dots represent finite parts of the integration, and \int^Λ defines an integral that is regulated in the ultraviolet by a cutoff Λ and whose infrared regularization (if any) is unspecified.

In order to simplify the notation we denote integrals that contain a product of the z functions by a \mathcal{W} . The first and second indices indicate the z -functions in the integrand, while the third index gives the power of q that resides in the denominator of the integrand, so

$$\mathcal{W}_{lmn} \equiv \frac{1}{\pi} \int^{\Lambda} dq \frac{z_l z_m}{q^n} . \quad (89)$$

In the same spirit of notational convenience and compactness we define:

$$\mathcal{Z}_{mn} \equiv \frac{1}{\pi} \int^{\Lambda} dq \frac{z_m}{q^n} . \quad (90)$$

All integrals \mathcal{W}_{lmn} and \mathcal{Z}_{mn} can be evaluated analytically, and this is done in Appendix A.

The divergences linear in Λ in Eq. (88) are then cancelled by requiring:

$$\mathcal{W}_{000}(\Lambda) + \frac{32h_{10}}{3\Lambda} \mathcal{Z}_{00}^2(\Lambda) = 0 . \quad (91)$$

Meanwhile, the divergence which is logarithmic in the cutoff is canceled by

$$\begin{aligned} \frac{2}{\sqrt{3}} \mathcal{W}_{001}(\Lambda) + \mathcal{W}_{011}(\Lambda) + \frac{16h_{11}}{3\Lambda^2} \mathcal{Z}_{00}^2(\Lambda) \\ + \frac{32h_{10}}{3\Lambda} \mathcal{Z}_{00}(\Lambda) \left(\frac{2}{\sqrt{3}} \mathcal{Z}_{01}(\Lambda) + \mathcal{Z}_{11}(\Lambda) \right) = 0 . \end{aligned} \quad (92)$$

By using the results for these integrals which are given in Appendix A¹ we derive the analytic forms for the NLO piece of the three-body force. First,

$$h_{10}(\Lambda) = - \frac{3\pi(1+s_0^2)}{64\sqrt{1+4s_0^2}} \frac{\sqrt{1+4s_0^2} - \cos(2s_0 \ln(\Lambda/\bar{\Lambda}) - \arctan 2s_0)}{\sin^2(s_0 \ln(\Lambda/\bar{\Lambda}) - \arctan s_0)} . \quad (93)$$

Since $\bar{\Lambda}$ is determined by the LO renormalization condition (e.g. $\bar{\Lambda} = 13.1\kappa_*$ in the unitary limit), Eq. (93) is a prediction for $h_{10}(\Lambda)$. Meanwhile, Eq. (92) gives

$$\begin{aligned} h_{11}(\Lambda) = & - \frac{\sqrt{3}\pi(1+s_0^2)}{16} \frac{(1+|C_{-1}|\cos(\arg C_{-1}))}{\sin^2(s_0 \ln(\Lambda/\bar{\Lambda}) - \arctan s_0)} \ln(\Lambda/\mu) \\ & + \frac{\sqrt{3}\pi(1+s_0^2)}{32s_0} \frac{\sin(2s_0 \ln(\Lambda/\bar{\Lambda})) + |C_{-1}|\sin(2s_0 \ln(\Lambda/\bar{\Lambda}) + \arg C_{-1})}{\sin^2(s_0 \ln(\Lambda/\bar{\Lambda}) - \arctan s_0)} \\ & - \frac{\sqrt{3}\pi(1+s_0^2)^{3/2}}{16s_0} \frac{\cos(s_0 \ln(\Lambda/\bar{\Lambda})) + |C_{-1}|\cos(s_0 \ln(\Lambda/\bar{\Lambda}) + \arg C_{-1})}{\sin^3(s_0 \ln(\Lambda/\bar{\Lambda}) - \arctan s_0)} \times \\ & \left[1 - \frac{1}{\sqrt{1+4s_0^2}} \cos(2s_0 \ln(\Lambda/\bar{\Lambda}) - \arctan(2s_0)) \right] \end{aligned} \quad (94)$$

¹ The result for, e.g. $\mathcal{Z}_{00}(\Lambda)$, would seem to neglect the effect of the infrared regularization, which could affect the answer for h_{11} . However, the combination of the infrared-regularization dependence of $\mathcal{Z}_{01}(\Lambda)$ and $\mathcal{Z}_{11}(\Lambda)$ is zero, and those of $\mathcal{W}_{001}(\Lambda)$ and $\mathcal{W}_{011}(\Lambda)$ can be absorbed into the numerically fitted parameter μ , which is included in $h_{11}(\Lambda)$.

The μ in Eq. (94) subsumes information on the finite part of $\mathcal{O}(\Lambda^0)$, and its value is determined by the renormalization conditions at NLO. Numerically this piece is of the same order as $\ln \Lambda$, as long as Λ is not extremely large.

We compare the analytical and numerical results for a particular renormalization condition in Figs. 5 and 6. Note that in order to do this comparison in Fig. 6 we have fitted the value of μ to the numerical results. However, the coefficient of the $\log(\Lambda/\mu)$ term in Eq. (94) is still predictive, and is confirmed by comparison to the numerical results. The analytic and numerical results agree to within our numerical accuracy of 10^{-3} when $\mu = 0.990\kappa_*$.

The renormalization condition chosen here is $\kappa_* = 1$ at LO and NLO, and $\gamma_0 = \kappa_*/0.316$ at NLO. This corresponds to a recombination minimum that receives no range corrections at NLO. The value of μ is affected by the choice of NLO renormalization conditions. We have checked that the numerical results for $h_{11}(\Lambda)$ obtained with other renormalization conditions can be well described by choosing alternative values of μ .

In both figures we plot the inverse $1/h_{10}$ and $1/h_{11}$ of the low-energy coefficients, and so the bumps that can be seen in Fig. 6 are the result of zeros in Eq. (94). The competition between the different terms in Eq. (94) is clearly seen in the comparison. In particular, the double pole has a coefficient which grows with $\ln \Lambda$, and this produces a turning point which is in increasing proximity to the position of the dominant triple pole as Λ grows.

In principle, the details of the regularization at NLO can affect the discrepancy between analytical expressions and numerical results in the NLO three-body force. In order to eliminate this effect, we first calculated the LO amplitude, t_0 , at a large cutoff, $\Lambda = 10^{12}\kappa_*$. Then we insert the resulted t_0 into NLO calculations integrated to a relatively smaller cutoff, $\Lambda < 10^6\kappa_*$, which suppresses the corrections from the details of the regularization to $< 10^{-6}$.

VI. UNIVERSAL RELATIONS AT NLO

In the limit $r_0/a = 0$, the two-body scattering lengths at which key experimental features occur, such as the atom-dimer resonance at positive scattering length $a = a_*$, the three-atom resonance at negative scattering length $a = a_-$, and the recombination minimum at $a = a_0$, obey a set of universal relations. Indeed, all three features can be related to the binding

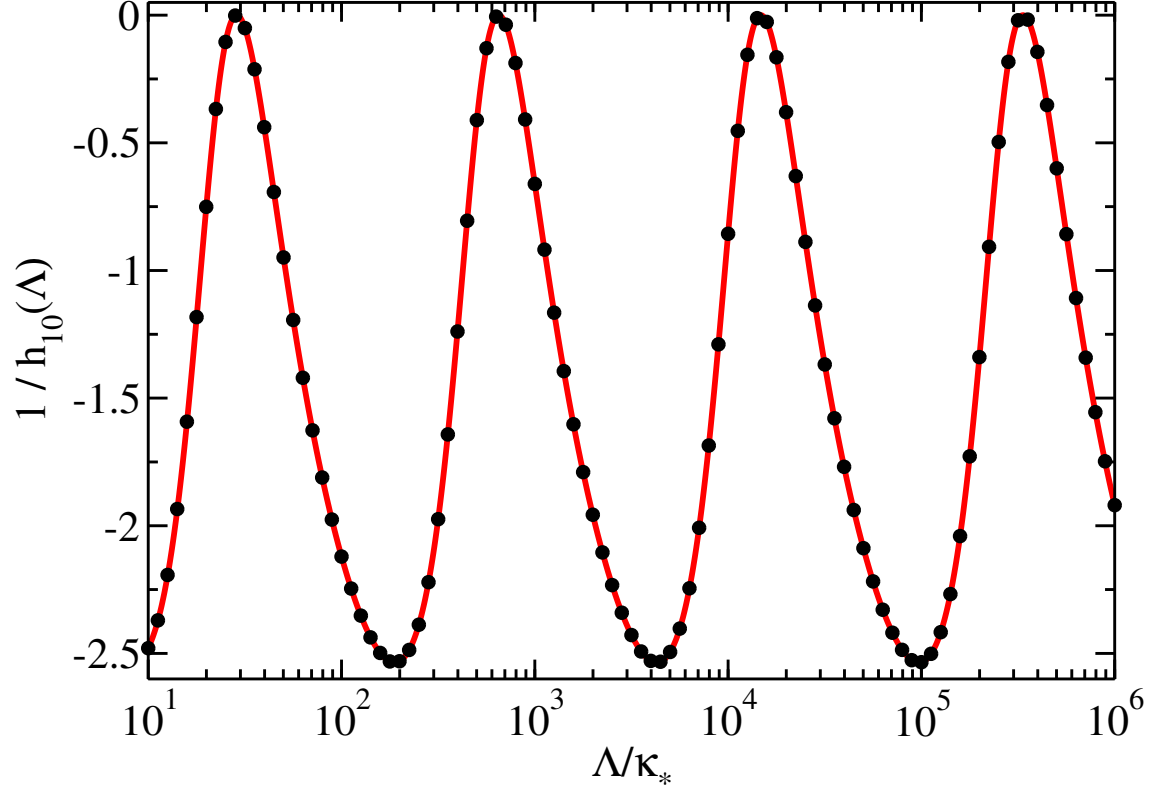


FIG. 5: $h_{10}(\Lambda)$: The dots are numerical results for h_{10} with the NLO calculation renormalized such that the LO prediction of $\kappa_* = 1$ ($\bar{\Lambda} = 13.1$) is maintained. The solid line (red) is the analytic function $h_{10}(\Lambda)$ given by Eq. (93) with the same parameter $\bar{\Lambda}$.

momentum of the three-atom state in the unitary limit, κ_* [13]:

$$a_* = 0.0708\kappa_*^{-1}, \quad (95)$$

$$a_- = -1.51\kappa_*^{-1}, \quad (96)$$

$$a_0 = 0.316\kappa_*^{-1}. \quad (97)$$

We can eliminate κ_* in the equations above and then rewrite them in terms of the inverse scattering length ($\gamma = 1/a$ at LO)

$$\gamma_* = \theta_*\gamma_0, \quad \gamma_- = \theta_-\gamma_0, \quad \kappa_* = \theta_\infty\gamma_0, \quad (98)$$

where $\theta_* = 4.47$, $\theta_- = -0.210$ and $\theta_\infty = 0.316$.

Once the two-body effective range, r_0 , is non-zero we can extend the LO universal relations such as Eq. (98) to include its effects. However, as shown above, these relations will now require two three-body parameters as input to predict a third one. This means that, before

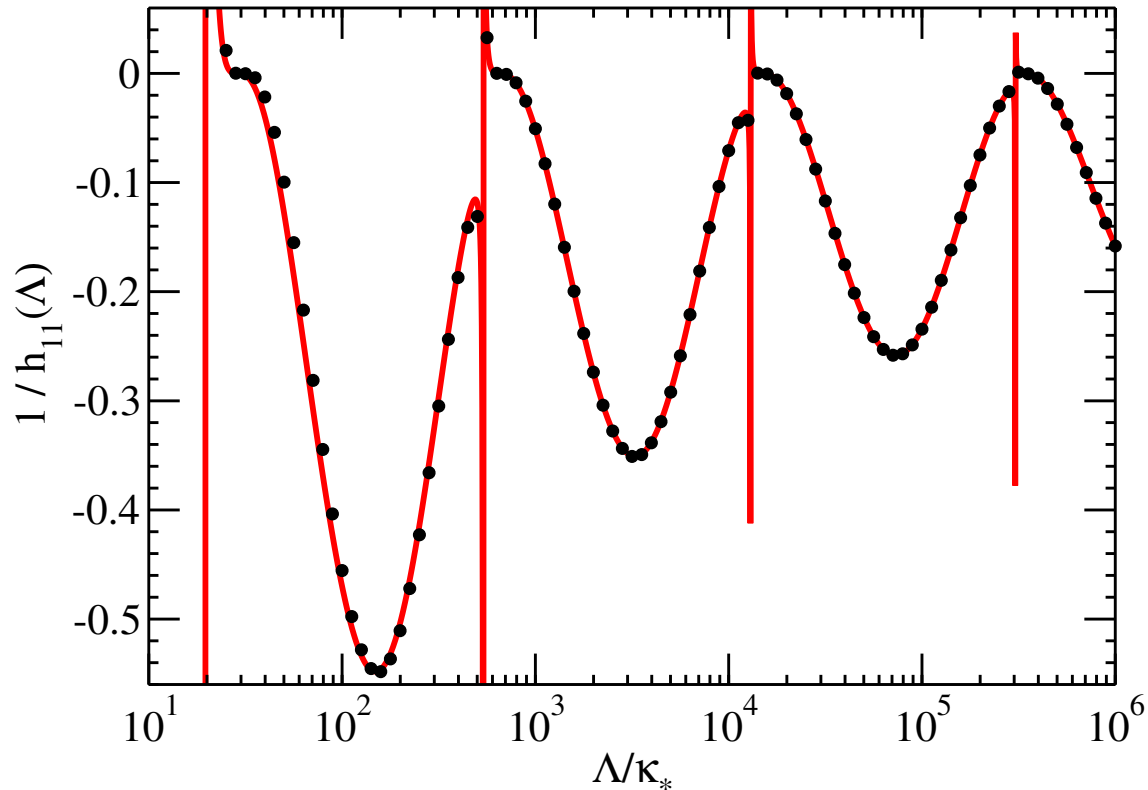


FIG. 6: $h_{11}(\Lambda)$: The dots are results of a numerical calculation of h_{11} with the additional NLO counterterm fitted to maintain the value of $\gamma_0 = \kappa_*/0.316$ predicted at LO. The LO renormalization condition, $\kappa_* = 1$ ($\bar{\Lambda} = 13.1$), is also kept at NLO. The solid line (red) is the analytic function $h_{11}(\Lambda)$ given by Eq. (94), with μ fitted to $0.99\kappa_*$ in order to obtain good agreement with the numerical values.

predictions can be made, two three-body observables have to be determined, either from experiment or from the underlying microscopic interaction that governs two- and three-body properties. To illustrate this, we assume that the positions of the two features γ_* and γ_0 are known. The effects of the effective range *perturbation* can then be included by adding a term linear in r_0 to the LO universal relation between γ_* and γ_0

$$\gamma_* = \theta_* \gamma_0 + r_0 \mathcal{I}_* \gamma_0^2. \quad (99)$$

The real and dimensionless number \mathcal{I}_* is non-universal in the sense that it depends on the renormalization condition, and thus on the type of physical system under consideration. The universal relations between other features are modified in the same way. For example

$$\Delta\gamma_- = r_0 \mathcal{I}_- \gamma_0^2, \quad (100)$$

where γ_- can be predicted if the relation between \mathcal{I}_* and \mathcal{I}_- is known. Similarly, the shift from the LO value of κ_* can be written as

$$\Delta\kappa_* = r_0\mathcal{I}_\infty\gamma_0^2 . \quad (101)$$

Note that in Eqs. (99)–(101) we have employed γ_0 to make up the dimensions of the NLO correction. This is a matter of convenience, since all dimensional quantities are related at LO by formulae such as Eqs. (95)–(97). We also used the fact that the NLO shifts in these three-body observables are strictly linear in r_0 in our perturbative analysis.

While the parameters that we have introduced above are not universal, the relations between them are. These are linear as a consequence of first-order perturbation theory. We have obtained these linear relations numerically and verified their stability for a wide range of possible renormalization conditions. In the case of the renormalization scheme discussed in the previous paragraph (γ_0 fixed at LO and NLO, and γ_* the additional input at NLO needed to fix h_{11}) we found

$$\begin{aligned} \mathcal{I}_- &= \xi_{-,*} + \eta_{-,*}\mathcal{I}_* , \\ \mathcal{I}_\infty &= \xi_{\infty,*} + \eta_{\infty,*}\mathcal{I}_* , \end{aligned} \quad (102)$$

with

$$\begin{aligned} \xi_{-,*} &= 0.256 , \\ \xi_{\infty,*} &= -0.286 , \\ \eta_{-,*} &= 1.65 \times 10^{-2} , \\ \eta_{\infty,*} &= -2.04 \times 10^{-2} . \end{aligned} \quad (103)$$

Combining Eqs. (99), (100), (101) and (102) with each other leads to relations that contain only observable features and the parameters in Eq. (103)

$$\gamma_- = \theta_- \gamma_0 + \xi_{-,*} r_0(a_-) \gamma_0^2 + \eta_{-,*} \frac{r_0(a_-)}{r_0(a_*)} (\gamma_* - \theta_* \gamma_0) , \quad (104a)$$

$$\kappa_* = \theta_\infty \gamma_0 + \xi_{\infty,*} r_0(a_\infty) \gamma_0^2 + \eta_{\infty,*} \frac{r_0(a_\infty)}{r_0(a_*)} (\gamma_* - \theta_* \gamma_0) . \quad (104b)$$

It is important to note at this point, that different universal relations can be generated depending on which three-body features are assumed to be known.

We can now apply our results to recent experimental measurements of recombination in ultracold gases. Lithium-7 atoms in the $|F = 1, m_F = 0\rangle$ hyperfine state are one system for which the scattering length and effective range are known as functions of the magnetic field. Gross *et al.* [23] measured a number of recombination features for this system. On the positive scattering length side of the resonance, they were able to measure a recombination minimum at $a_0 \approx 1160a_B$ and the position of an atom-dimer resonance at $a_* \approx 290a_B$. On the negative scattering length side, they measured a recombination maximum $a_-^{(-)} \approx -264a_B$. The superscript $(-)$ indicates that this a_- represents the point where the next deeper trimer branch relative to a_0 and a_* crosses the three-atom threshold. Ref. [23] also contains the results of a calculation for the magnetic field dependence of scattering length a and effective range r_0 . We will employ these results to illustrate the use of the relations presented above.

The values of the effective range at the scattering lengths where experimental features occur are

$$\begin{aligned} r_0(a_0) &= -34.5a_B \\ r_0(a_*) &= -74.7a_B \\ r_0\left(a_-^{(-)}\right) &= 27.2a_B, \end{aligned}$$

We now use the values of two of these observables to *predict* the third one (whose measurement was already reported in Ref. [23]). In particular, we will predict a_* after renormalizing to a_0 and $a_-^{(-)}$. In doing this we assume that the low-energy constants H_0 , h_{10} , and h_{11} depend only weakly on the magnetic field and are the same for all three experimental features we consider. We start out again by relating the known features through the LO universal relations and a shift linear in the effective range times a non-universal number that contains the information about the NLO renormalization condition

$$\gamma_0 = -0.210\gamma_-^{(-)} + r_0(a_0) \cdot \mathcal{I}_0^{(-)} \gamma_-^{(-)2}, \quad (105a)$$

$$\gamma_* = -0.939\gamma_-^{(-)} + r_0(a_*) \cdot \mathcal{I}_*^{(-)} \gamma_-^{(-)2}, \quad (105b)$$

We again can numerically extract the universal parameters that relate the parameters $\mathcal{I}_0^{(-)}$ and $\mathcal{I}_*^{(-)}$ via

$$\mathcal{I}_*^{(-)} = -0.309 + 7.17 \mathcal{I}_0^{(-)}, \quad (106)$$

here we haven chosen to write out the numerical values of the universal parameters directly to avoid notational clutter. We can then combine these equations into one universal relation that predicts the position of a_* .

The corresponding universal relation is given by

$$\gamma_* = \theta_*^{(-)} \gamma_-^{(-)} - 0.309 r_0(a_*) \gamma_-^{(-)2} + 7.17 \frac{r_0(a_*)}{r_0(a_0)} \left(\gamma_0 - \theta_0^{(-)} \gamma_-^{(-)} \right) \quad (107)$$

where the parameters of the universal LO relations are given by $\theta_*^{(-)} = -0.939$ and $\theta_0^{(-)} = -0.210$.

We can alternatively generate a relation that gives the NLO result for γ_* as the relative shift to the LO universal equation between γ_* and γ_0 .

$$\gamma_* = \theta_* \gamma_0 - 7.02 r_0(a_*) \gamma_0^2 + 0.566 \frac{r_0(a_*)}{r_0(a_-^{(-)})} \left(\gamma_-^{(-)} - \theta_-^{(+)} \gamma_0 \right) \quad (108)$$

where $\theta_* = 4.47$, $\theta_-^{(+)} \equiv 1/\theta_0^{(-)} = -4.75$ and we have again immediately inserted the numerical values of the NLO universal parameters. Equations (107) and (108) will generally give different numerical results for γ_* which provides a lower bound on higher order corrections.

Using the numerical values for the positions of three-body features and the numerical values for the effective ranges, we obtain

$$a_* = (271 - 108 + \dots) a_B , \quad (109)$$

$$a_* = (257 - 2 + \dots) a_B , \quad (110)$$

from Eq. (107) and Eq. (108), respectively.

Our predictions of a_* in both renormalization schemes are consistent with our previous findings [9]. Combining both results and including a conservative estimate of higher order corrections, we obtain therefore the same result as quoted in Ref. [9]

$$a_* = (210 \pm 44) a_B . \quad (111)$$

VII. CONCLUSION

In this work we have presented a perturbative calculation of next-to-leading order (in $\ell/|a|$) corrections to universal three-body physics. We have shown that an additional three-body counterterm is required for renormalization if and only if scattering-length-dependent

quantities are considered. The inverse scattering length therefore plays a similar role in the SREFT to that of the pion mass in chiral perturbation theory. Counterterms proportional to the inverse of the scattering length occur at orders beyond leading, and these must be fitted by considering scattering-length-dependent data.

The advantages of the perturbative analysis we have presented here are twofold. First, it allowed us to derive analytic expressions for the next-to-leading-order shifts of resonance positions in recombination experiments. Second, it permitted an explicit treatment of the renormalization of divergent integrals while keeping the LO counterterm fixed. This produced analytic forms for the running of the NLO pieces of the three-body force.

Our analysis is applicable to systems for which the scattering length and effective range are known as a function of the magnetic field. If data on three-body processes at different values of the two-body scattering length exists then effective-range corrections to recombination features can be treated in the manner described above. Data from the Bar-Ilan and Rice groups [23, 24] on Lithium-7 recombination were recently analyzed in this way [9].

A calculation of the divergence structure of bosonic observables in SREFT at next-to-next-to-leading order $\mathcal{O}(\ell^2/a^2)$ is underway [25].

Acknowledgments

We thank Eric Braaten and Hans-Werner Hammer for useful discussions. DRP and CJ are grateful for the hospitality of the HISKP at the University of Bonn, and also thank the Institute for Nuclear Theory at the University of Washington for its hospitality during the INT program 10-01 “Simulations and Symmetries: Cold Atoms, QCD, and Few-nucleon Systems”. Parts of this work were done in each of these venues. This work was supported by the US Department of Energy under contracts DE-FG02-93ER40756 and DE-FG02-00ER41132, the Swedish Research Council (LP) and by a Mercator Fellowship (DRP).

Appendix A: Relevant Integrals

The following functions are used in the derivation of the analytical expression for the NLO three-body counterterms h_{10} and h_{11} .

$$\mathcal{Z}_{00} = \frac{1}{\pi} \int^{\Lambda} dq z_0 = \frac{1}{\pi} \int^{\Lambda} dq \sin \left(s_0 \ln \frac{q}{\Lambda} \right) = \frac{\Lambda}{\pi \sqrt{1+s_0^2}} \sin \left(s_0 \ln \frac{\Lambda}{\Lambda} - \arctan s_0 \right), \quad (\text{A1})$$

$$\mathcal{Z}_{01} = \frac{1}{\pi} \int^{\Lambda} dq \frac{z_0}{q} = \frac{1}{\pi} \int^{\Lambda} \frac{dq}{q} \sin \left(s_0 \ln \frac{q}{\Lambda} \right) = -\frac{1}{\pi s_0} \cos \left(s_0 \ln \frac{\Lambda}{\Lambda} \right), \quad (\text{A2})$$

$$\begin{aligned} \mathcal{Z}_{11} &= \frac{1}{\pi} \int^{\Lambda} dq \frac{z_1}{q} = \frac{2|C_{-1}|}{\sqrt{3}\pi} \int^{\Lambda} \frac{dq}{q} \sin \left(s_0 \ln \frac{q}{\Lambda} + \arg C_{-1} \right) \\ &= -\frac{2|C_{-1}|}{\sqrt{3}\pi s_0} \cos \left(s_0 \ln \frac{\Lambda}{\Lambda} + \arg C_{-1} \right). \end{aligned} \quad (\text{A3})$$

Integrals that contain a product of the z functions are denoted by \mathcal{W} . The first and second index indicates the order of the two z -functions in the integrand's numerator, and the third index gives power of q in its denominator. I.e.

$$\begin{aligned} \mathcal{W}_{000} &= \frac{1}{\pi} \int^{\Lambda} dq z_0^2 = \frac{1}{2\pi} \int^{\Lambda} dq \left[1 - \cos \left(2s_0 \ln \frac{q}{\Lambda} \right) \right] \\ &= \frac{\Lambda}{2\pi} \left[1 - \frac{1}{\sqrt{1+4s_0^2}} \cos \left(2s_0 \ln \frac{\Lambda}{\Lambda} - \arctan(2s_0) \right) \right], \end{aligned} \quad (\text{A4})$$

$$\begin{aligned} \mathcal{W}_{001} &= \frac{1}{\pi} \int^{\Lambda} dq \frac{z_0^2}{q} = \frac{1}{2\pi} \int^{\Lambda} \frac{dq}{q} \left[1 - \cos \left(2s_0 \ln \frac{q}{\Lambda} \right) \right] \\ &= \frac{1}{2\pi} \left[\ln \Lambda - \frac{1}{2s_0} \sin \left(2s_0 \ln \frac{\Lambda}{\Lambda} \right) \right], \end{aligned} \quad (\text{A5})$$

$$\begin{aligned} \mathcal{W}_{011} &= \frac{1}{\pi} \int^{\Lambda} dq \frac{z_0 z_1}{q} = \frac{|C_{-1}|}{\sqrt{3}\pi} \int^{\Lambda} \frac{dq}{q} \left[\cos(\arg C_{-1}) - \cos \left(2s_0 \ln \frac{q}{\Lambda} + \arg C_{-1} \right) \right] \\ &= \frac{|C_{-1}|}{\sqrt{3}\pi} \left[\cos(\arg C_{-1}) \ln \Lambda - \frac{1}{2s_0} \sin \left(2s_0 \ln \frac{\Lambda}{\Lambda} + \arg C_{-1} \right) \right]. \end{aligned} \quad (\text{A6})$$

Appendix B: Parameterization of the three-body spectrum on the negative-scattering-length side

We follow Ref. [13] and define B_0 on the negative γ side as

$$B_0(\gamma) = -\gamma^2 \mathcal{G} \left(\frac{\gamma}{\gamma_-} \right), \quad (\text{B1})$$

where the dimensionless function $\mathcal{G}(1) = 0$ at threshold. By substituting this into Eq. (79) we have

$$\Delta\gamma_- = \frac{B_1(\gamma_-)}{\gamma_- \mathcal{G}'(1)}. \quad (\text{B2})$$

The calculation of $\Delta\gamma_-$ is numerically accurate because $\mathcal{G}'(1) \neq 0$. We find $\mathcal{G}'(1) = 0.98$. That $\mathcal{G}'(1) \neq 0$ is supported by the empirical fitting formula in [13] near $\gamma = \gamma_-$, where κ and γ obey Eq. (67), while the function $\Delta(\xi)$ obeys a different expression from Eq. (68), because now we are near the three-atom resonance, not the atom-dimer resonance, which is indicated by $\xi = -\pi$:

$$\xi \in \left[-\pi, -\frac{5\pi}{8} \right] : \Delta = -0.89 + 0.28z + 0.25z^2$$

$$z = (\pi + \xi)^2 \exp[-1/(\pi + \xi)^2], \quad (\text{B3})$$

$dB_0/d\gamma$ in this region is

$$\frac{dB_0}{d\gamma} = \frac{2H \sin \xi \left(\frac{1}{2s_0} \frac{d\Delta}{d\xi} \sin \xi + \cos \xi \right)}{\frac{1}{2s_0} \frac{d\Delta}{d\xi} \cos \xi - \sin \xi}, \quad (\text{B4})$$

whose numerator and denominator both go to zero when $\xi \rightarrow -\pi$. After applying L'Hôpital's rule we calculate $dB_0/d\gamma$ at γ_- :

$$\left. \frac{dB_0}{d\gamma} \right|_{\gamma=\gamma_-} = \left. \frac{2H}{1 - \frac{1}{2s_0} \frac{d^2\Delta}{d\xi^2}} \right|_{\xi=-\pi}. \quad (\text{B5})$$

Equation (B3) indicates that $d^2\Delta/d\xi^2 = 0$ at $\xi = -\pi$, therefore

$$\left. \frac{dB_0}{d\gamma} \right|_{\gamma=\gamma_-} = 2H = -2\gamma_-, \quad (\text{B6})$$

and so

$$\mathcal{G}'(1) = 2. \quad (\text{B7})$$

Thus, the function $\mathcal{G}'(1)$ is finite and nonzero from the empirical fitting formula in [13]. However, the value in Eq. (B7) is larger than the correct numerical value in Eq. (B7).

-
- [1] V. Efimov, Phys. Lett., **33B**, 563 (1970).
 - [2] H.-W. Hammer and L. Platter, Ann. Rev. Nucl. Part. Sci. **60**, 207-236 (2010).
 - [3] P. F. Bedaque, H. W. Hammer and U. van Kolck, Phys. Rev. Lett., **82**, 463 (1999).
 - [4] P. F. Bedaque, H.-W. Hammer, and U. van Kolck, Nucl. Phys. A, **646**, 444 (1999).
 - [5] H.-W. Hammer and T. Mehen. Phys. Lett. B, **516**, 353 (2001).

- [6] P. F. Bedaque, G. Rupak, H. W. Griesshammer, and H.-W. Hammer. Nucl. Phys. A, **714**, 589 (2003).
- [7] L. Platter and D. R. Phillips, Few Body Syst. **40**, 35 (2006).
- [8] L. Platter, C. Ji and D. R. Phillips. Phys. Rev. A, **79**, 022702 (2009).
- [9] C. Ji, D. R. Phillips and L. Platter, Europhys. Lett. **92**, 13003 (2010)
- [10] S. R. Beane, P. F. Bedaque, W. C. Haxton, D. R. Phillips, and M. J. Savage, “From hadrons to nuclei: Crossing the border,” in the Borris Ioffe Festschrift, “At the frontier of particle physics: handbook of QCD”, M. Shifman (ed.).
- [11] P. F. Bedaque and U. van Kolck, Ann. Rev. Nucl. Part. Sci., **52**, 339 (2002).
- [12] P. F. Bedaque and H. W. Griesshammer, Nucl. Phys. **A671**, 357-379 (2000).
- [13] E. Braaten and H. -W. Hammer, Phys. Rept. **428**, 259-390 (2006).
- [14] E. Braaten, M. Kusunoki, D. Zhang, Annals Phys. **323**, 1770-1815 (2008).
- [15] D. B. Kaplan, Nucl. Phys. **B494**, 471-484 (1997).
- [16] U. van Kolck, Nucl. Phys. A **645** (1999) 273.
- [17] D. B. Kaplan, M. J. Savage and M. B. Wise, Phys. Lett. B **424** (1998) 390.
- [18] D. B. Kaplan, M. J. Savage and M. B. Wise, Nucl. Phys. B **534** (1998) 329.
- [19] J. Gegelia, Phys. Lett. B **429** (1998) 227.
- [20] M. C. Birse, J. A. McGovern and K. G. Richardson, Phys. Lett. B **464** (1999) 169.
- [21] E. Braaten, D. Kang and L. Platter, Phys. Rev. Lett. **106**, 153005 (2011).
- [22] G.V. Skorniakov and K.A. Ter-Martirosian, Sov. Phys. JETP **4**, 648 (1957) [J. Exptl. Theoret. Phys. (U.S.S.R.) **31**, 775 (1956)].
- [23] N. Gross, Z. Shotan, S. Kokkelmans and L. Khaykovich, Phys. Rev. Lett., **103**, 163202 (2009).
- [24] S. E. Pollack, D. Dries and R. G. Hulet, Science, **326**, 1683 (2009).
- [25] C. Ji and D. R. Phillips, in preparation.